A fully fermionic mean field theory of the cuprate superconductors

Tiago C. Ribeiro and Xiao-Gang Wen
Department of Physics, Massachusetts Institute of Technology, Cambridge, Massachusetts 02139, USA
(Dated: October 31, 2004)

We introduce a new mean field approach to the extended tJ model that incorporates both electron-like quasiparticle and spin-charge separated excitations as suggested by experiments and numerical studies. It leads to a mean field phase diagram which is consistent with that of hole and electron doped cuprates. Moreover, it provides a framework to describe the observed evolution of the electron spectral function from the undoped insulator to the overdoped Fermi metal for both hole and electron doping. The theory also provides a non-BCS mechanism leading to superconductivity.

arXiv:cond-mat/0410750 v1 28 Oct 2004

The evolution of the electronic structure from the undoped antiferromagnetic (AF) insulator to the overdoped metallic state of cuprates is a long standing problem. The plethora of anomalous behavior displayed by these materials is particularly striking in hole underdoped samples, for which both experimental [1–6] and numerical [7–9] evidence suggests a dichotomy of the electronic excitations: the excitations around the nodal points [$\boldsymbol{k} = (\pm\frac{\pi}{2}, \pm\frac{\pi}{2})$] are well described as Landau's quasiparticles while those near the anti-nodal points [$\boldsymbol{k} = (\pi, 0), (0, \pi)$] show no signs of quasiparticle-like behavior. Some experimental [10] and numerical [7–9, 11] studies relate this absence of quasiparticles to spin-charge separation phenomenology.

In the slave-boson approach to the tJ model [12] the electron is split into a spinon (a spin-1/2 neutral fermion) and a holon (a spin-0 charged boson). The spin-charge separation phenomenon corresponds to the rapid decay of an electron excitation into a spinon and a holon, leading to the lack of quasiparticle features as observed near the anti-nodal points. However, the appearance of quasiparticles near the nodal points means that, in this $\boldsymbol{k}$-space region, the spinon and the holon form a bound state. [12, 13] Within the slave-boson theory this fact can only be captured by going beyond the mean field (MF) approximation.

In order to overcome the above shortcoming, in this letter, a new approach to the extended tJ model is introduced. Instead of using spinons and holons, the resulting new MF theory describes the low energy physics in terms of spinons and doped carriers. The doped carriers are holes in the hole doped (HD) regime and electrons in the electron doped (ED) regime. For ease of speaking, below we refer to the doped holes/electrons as dopons, which are spin-1/2 charged fermions. A holon is then viewed as a bound state of a spinon and a dopon. We show that the new MF approach leads to a MF phase diagram that resembles the one of HD and ED cuprates. It also accounts for the doping evolution of the electronic structure, as seen by ARPES, in both HD and ED samples.

We start with the 2D $tt't''J$ Hamiltonian

$$H_{tJ} = J \sum_{\langle ij\rangle \in NN} \boldsymbol{S}_i.\boldsymbol{S}_j - \sum_{\langle ij\rangle,\sigma} t_{ij} \mathcal{P} \left(c^\dagger_{i,\sigma} c_{j,\sigma} + H.c. \right) \mathcal{P} \quad (1)$$

where $t_{ij} = t, t', t''$ for first, second and third nearest neighbor (NN) sites respectively and $\mathcal{P}$ projects out doubly occupied sites. The tJ-model on-site Hilbert space, $\{|\uparrow\rangle, |\downarrow\rangle, |0\rangle\}$, includes states with either one or zero spin-$\frac{1}{2}$ objects.

To obtain the new MF theory we start with an enlarged on-site Hilbert space $\{|\uparrow 0\rangle, |\downarrow 0\rangle, |\uparrow\uparrow\rangle, |\uparrow\downarrow\rangle, |\downarrow\uparrow\rangle, |\downarrow\downarrow\rangle\}$ which contains either one or two spin-$\frac{1}{2}$ objects. The states $|\uparrow 0\rangle$, $|\downarrow 0\rangle$ and the local singlet state $\frac{1}{\sqrt{2}}(|\uparrow\downarrow\rangle - |\downarrow\uparrow\rangle)$ map onto the states $|\uparrow\rangle$, $|\downarrow\rangle$ and the vacancy state $|0\rangle$, respectively, in the tJ-model on-site Hilbert space. The on-site triplet states, such as $\frac{1}{\sqrt{2}}(|\uparrow\downarrow\rangle + |\downarrow\uparrow\rangle)$, are unphysical. We also introduce the fermionic representation for the first spin (the lattice spin), $\boldsymbol{S}_i = \frac{1}{2} f^\dagger_i \boldsymbol{\sigma} f_i$, and the second spin (the doped spin), $\frac{1}{2} d^\dagger_i \boldsymbol{\sigma} d_i$, where $\boldsymbol{\sigma}$ are the Pauli matrices. Here, $f^\dagger_i$ and $d^\dagger_i$ are the spinon and the dopon creation operators. Then, the Hamiltonian $H^{enl}_{tJ} = H^t_{enl} + H^J_{enl}$, where

$$\begin{aligned} H^t_{enl} &= \sum_{\langle ij\rangle,\sigma} t_{ij} \widetilde{\mathcal{P}} \left[\left(d^\dagger_i \boldsymbol{\sigma} d_j \right) . \left(i \boldsymbol{S}_i \times \boldsymbol{S}_j - \frac{\boldsymbol{S}_i + \boldsymbol{S}_j}{2} \right) + \right. \\ &\qquad \left. + \frac{1}{4} d^\dagger_i d_j + d^\dagger_i d_j \boldsymbol{S}_i.\boldsymbol{S}_j + h.c. \right] \widetilde{\mathcal{P}} \ , \\ H^J_{enl} &= J \sum_{\langle ij\rangle \in nn} \boldsymbol{S}_i.\boldsymbol{S}_j \, \widetilde{\mathcal{P}} \left(1 - d^\dagger_i d_i \right) \left(1 - d^\dagger_j d_j \right) \widetilde{\mathcal{P}} \end{aligned} \quad (2)$$

and $\widetilde{\mathcal{P}}$ enforces the no double occupancy constraint for the d-fermion, equals H_{tJ} in the tJ-model Hilbert space. H^t_{enl} is such that only local singlet states hop between different lattice sites whereas local triplet states have no kinetic energy. Therefore, *the dynamics enclosed in H^t_{enl} effectively implements the local singlet constraint.* We are mostly interested in the low doping regime and, thus, below we drop the projection operators $\widetilde{\mathcal{P}}$ in H^{enl}_{tJ}.

The Hamiltonian H^{enl}_{tJ} is a sum of terms with up to six fermion operators. In the following, we replace some multiple-fermion operators by their average so that the resulting MF Hamiltonian is quadratic in the operators $f^\dagger$, f, $d^\dagger$ and d and describes the hopping, pairing and mixing of spinons and dopons.

The exchange Hamiltonian H^J_{enl} is decoupled by means of the d-wave ansatz [12] and becomes $-\frac{3\tilde{J}}{8} \sum_{\langle ij\rangle \in NN} [\chi f^\dagger_i f_j + (-)^{j_y - i_y} \Delta (f^\dagger_{i\uparrow} f^\dagger_{j\downarrow} - f^\dagger_{i\downarrow} f^\dagger_{j\uparrow}) +$

$h.c.] + a_0 \sum_i (f_i^\dagger f_i - 1)$ where $\tilde{J} = (1-x)^2 J$, χ and Δ are the spinon bond and pairing MFs and a_0 is the Lagrange multiplier enforcing $\langle f_i^\dagger f_i \rangle = 1$.

We now consider the hopping Hamiltonian H^t_{enl}. Once the effective hopping amplitude of one hole in an AF background is renormalized by the spin fluctuations, [14] we replace the bare t, t' and t'' by the effective hopping parameters t_1, t_2 and t_3 which are determined phenomenologically. The terms $[(d_i^\dagger \boldsymbol{\sigma} d_j).(i\boldsymbol{S}_i \times \boldsymbol{S}_j)]$ and $(d_i^\dagger d_j \boldsymbol{S}_i.\boldsymbol{S}_j)$ in H^t_{enl} are the sum of operators like $d^\dagger_{i,\alpha} d_{j,\beta} f^\dagger_{i,\gamma} f_{j,\delta} f^\dagger_{j,\mu} f_{i,\nu}$ and, in our decoupling scheme, only contribute to the MF spinon and dopon hopping terms. The first contribution comes from the averages of two d and two f operators ($\langle d^\dagger_{i,\alpha} d_{j,\beta} f^\dagger_{i,\gamma} f_{j,\delta} \rangle$) and yields the spinon NN hopping term $\frac{t_1 x}{2} \sum_{\langle ij \rangle \in NN} (f_i^\dagger f_j + h.c.)$. The second contribution arises, instead, from taking the averages of the four f operators ($\langle f^\dagger_{i,\gamma} f_{j,\delta} f^\dagger_{j,\mu} f_{i,\nu} \rangle$), which reduce to $\langle \boldsymbol{S}_i \times \boldsymbol{S}_j \rangle$ and $\langle \boldsymbol{S}_i.\boldsymbol{S}_j \rangle$, and adds up to the dopon hopping term. We remark that, in the presence of *local* AF correlations, the vacancy in the hole/electron-like quasiparticle state is surrounded by an AF-like configuration of spins. [9] To approximately account for this effect, we assume that the spins encircling the vacancy in the one-dopon state are in a *local* Néel configuration. Therefore we use $\langle \boldsymbol{S}_i \times \boldsymbol{S}_j \rangle = 0$ and $\langle 4\boldsymbol{S}_i.\boldsymbol{S}_j \rangle = (-1)^{j_x + j_y - i_x - i_y}$. Finally, to decouple the spinon-dopon interaction $[(d_i^\dagger \boldsymbol{\sigma} d_j).(\boldsymbol{S}_i + \boldsymbol{S}_j)]$ we introduce $b_0 = \langle f_i^\dagger d_i \rangle$ and $b_1 = \langle \frac{3}{8} \sum_\nu t_\nu \sum_{\hat{u} \in \nu\, NN} f_i^\dagger d_{i+\hat{u}} \rangle$, where $\hat{u} = \pm\hat{x}, \pm\hat{y}$, $\hat{u} = \pm\hat{x} \pm \hat{y}$ and $\hat{u} = \pm 2\hat{x}, \pm 2\hat{y}$ for $\nu = 1, 2, 3$ respectively.

The resulting total MF Hamiltonian, written in terms of the Nambu operators $\eta_i^\dagger = [\eta_{i1}^\dagger \eta_{i2}^\dagger] = [d_{i\uparrow}^\dagger d_{i\downarrow}]$ and $\psi_i^\dagger = [\psi_{i1}^\dagger \psi_{i2}^\dagger] = [f_{i\uparrow}^\dagger f_{i\downarrow}]$, is:

$$H^{MF}_{tJ} = \sum_{\boldsymbol{k}} \left[\begin{array}{cc} \psi^\dagger_{\boldsymbol{k}} & \eta^\dagger_{\boldsymbol{k}} \end{array} \right] \left[\begin{array}{cc} \alpha^z_{\boldsymbol{k}} \sigma_z + \alpha^x_{\boldsymbol{k}} \sigma_x & \beta_{\boldsymbol{k}} \sigma_z \\ \beta_{\boldsymbol{k}} \sigma_z & \gamma_{\boldsymbol{k}} \sigma_z \end{array} \right] \left[\begin{array}{c} \psi_{\boldsymbol{k}} \\ \eta_{\boldsymbol{k}} \end{array} \right] + \frac{3\tilde{J}N}{4}(\chi^2 + \Delta^2) - 2Nb_0 b_1 - N\mu_d \quad (3)$$

where $\alpha^z_{\boldsymbol{k}} = -(\frac{3\tilde{J}}{4}\chi - t_1 x)(\cos k_x + \cos k_y) + a_0$, $\alpha^x_{\boldsymbol{k}} = -\frac{3\tilde{J}}{4}\Delta(\cos k_x - \cos k_y)$, $\beta_{\boldsymbol{k}} = \frac{3b_0}{4}[t_1(\cos k_x + \cos k_y) + 2t_2 \cos k_x \cos k_y + t_3(\cos 2k_x + \cos 2k_y)] + b_1$ and $\gamma_{\boldsymbol{k}} = 2t_2 \cos k_x \cos k_y + t_3(\cos 2k_x + \cos 2k_y) - \mu_d$, N is the lattice size and μ_d is the dopon chemical potential that sets the doping level $\langle d_i^\dagger d_i \rangle = x$. The eigenenergies of H^{MF}_{tJ} are $\epsilon^\pm_{1,\boldsymbol{k}} = \pm\sqrt{\rho_{\boldsymbol{k}} - \sqrt{\delta_{\boldsymbol{k}}}}$ and $\epsilon^\pm_{2,\boldsymbol{k}} = \pm\sqrt{\rho_{\boldsymbol{k}} + \sqrt{\delta_{\boldsymbol{k}}}}$ where $\delta_{\boldsymbol{k}} = \beta^2_{\boldsymbol{k}}[(\gamma_{\boldsymbol{k}} + \alpha^z_{\boldsymbol{k}})^2 + (\alpha^x_{\boldsymbol{k}})^2] + \frac{1}{4}[\gamma^2_{\boldsymbol{k}} - (\alpha^x_{\boldsymbol{k}})^2 - (\alpha^z_{\boldsymbol{k}})^2]^2$ and $\rho_{\boldsymbol{k}} = \beta^2_{\boldsymbol{k}} + \frac{1}{2}[\gamma^2_{\boldsymbol{k}} + (\alpha^x_{\boldsymbol{k}})^2 + (\alpha^z_{\boldsymbol{k}})^2]$. $\epsilon_{1,\boldsymbol{k}}$ and $\epsilon_{2,\boldsymbol{k}}$ are the lowest and highest energy bands respectively.

If we ignore the spinon-dopon mixing, the spinon sector of H^{MF}_{tJ} describes the same spin dynamics as the slave-boson theory. [13] The dopon sector, on the other hand, determines the dynamics of the hole/electron-like quasiparticle excitations. In the current approximation, the dopon only has intrasublattice hopping processes (see

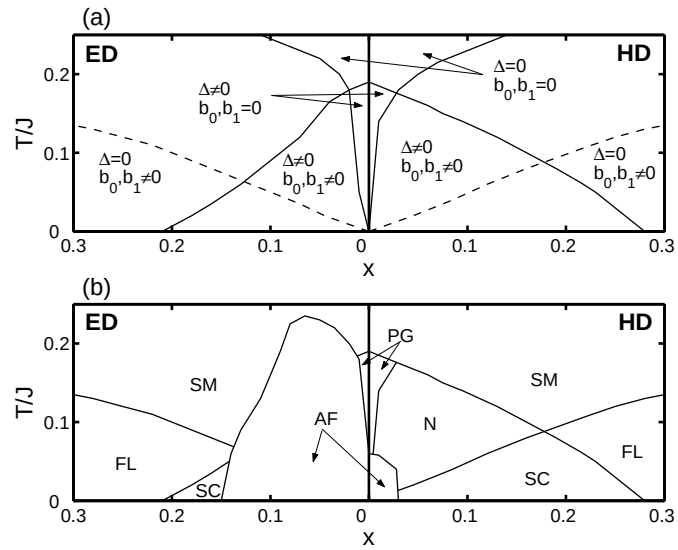

FIG. 1: (a) Regions in the (x-T) plane where $\Delta = 0$ or $\Delta \neq 0$ as well as $b_0 = b_1 = 0$ or $b_0, b_1 \neq 0$. The dashed lines indicate the T_{KT} described in the main text where long range order in the dopon-spinon mixing channel is destroyed by vortex fluctuations. (b) The (x-T) phase diagram including the AF, SC, strange metal (SM), Fermi liquid (FL) and pseudo-gap with and without Nernst signal, labeled by N and PG respectively, regions. Both HD and ED cases are depicted in (a) and (b).

$\gamma_{\boldsymbol{k}}$) due to the AF correlations enclosed in the spin average $\langle \boldsymbol{S}_i.\boldsymbol{S}_j \rangle$ used to derive H^{MF}_{tJ}. In the HD regime, we choose t_2 and t_3 so that $\gamma_{\boldsymbol{k}}$ approximately follows the high energy dispersion identified by ARPES [4, 15] which, for $x \approx 0$, is isotropic around $(\frac{\pi}{2}, \frac{\pi}{2})$ with a bandwith $\sim 2J$ and whose high energy pseudogap around $(\pi, 0)$ closes at $x \sim 0.3$. [1] As a result, $t_2^{HD} = 0.5 \times \frac{x}{0.3} J$ and $t_3^{HD} = 0.5J - 0.25 \times \frac{x}{0.3} J$. In ED materials the electron pocket shows up around $(\pi, 0)$ instead [16] and we take $t_2^{ED} = 0.8J - 0.3 \times \frac{x}{0.3} J$ and $t_3^{ED} = 0.10J + 0.15 \times \frac{x}{0.3} J$. The renormalized NN electron hopping amplitude t_1 is chosen to be $t_1 = -J$ as, we find, it correctly leads to the doping independent nodal dispersion "kink" energy $\approx \frac{J}{2}$ found in HD samples. [17]

After determining $t_{1,2,3}$ from the ARPES data, we calculated the MF phase diagram in Fig. 1a. It contains four MF phases, all of which are observed in the cuprates: (a) d-wave SC state when $b_0, b_1 \neq 0$ and $\Delta \neq 0$; (b) Fermi liquid state when $b_0, b_1 \neq 0$ and $\Delta = 0$; (c) pseudo-gap metal when $b_0, b_1 = 0$ and $\Delta \neq 0$; (d) strange metal when $b_0, b_1 = 0$ and $\Delta = 0$.

We note that the MF SC transition temperature is very high in the underdoped regime. This is an artifact of the MF calculation since the thermal fluctuations of the phases of the condensates $b_{0,1}$ are ignored. To crudely estimate the strength of the phase fluctuations of b_0, we note that the NN electron hopping term in H_{tJ} induces a term $-|t_1|\chi \sum_{<ij>} (b^*_{0i} b_{0j} + h.c.)$.

The resulting Kosterlitz-Thouless transition temperature $T_{KT} = 1.8|t_1|\chi b_0^2$, [18] above which the condensate average $\langle b_0 \rangle$ vanishes due to phase fluctuations, is plotted as the dashed-line in Fig. 1a. The state with long-range SC order only appears below T_{KT} (see Fig. 1b). Above T_{KT}, and in the underdoped regime, there appear two distinct pseudo-gap metal regions marked by N and PG in Fig. 1b. In region N, which is located between the MF T_c and T_{KT}, the non-vanishing magnitude of the MF order parameters $b_{0,1}$ leads to short-range SC correlations. This regime is observed experimentally, as suggested by the large Nernst signal measured in underdoped HD materials far above T_c. [19, 20] In the PG region $b_{0,1} = 0$ and the SC fluctuations become too small to be detected.

In the above MF calculation we have ignored the AF phase. To include this state we further introduce the MF decoupling channels $m = (-)^{i_x+i_y}\langle S_i^z \rangle$ and $n = -\frac{(-)^{i_x+i_y}}{8}\langle \sum_{\nu=2,3} t_\nu \sum_{\hat{u}\in\nu\, NN} d_i^\dagger \sigma_z d_{i+\hat{u}} + h.c.\rangle$ that account for the staggered magnetization in the lattice spin and dopon systems respectively. We thus add $2J^* N m^2 - 4Nmn - 2(J^* m - n)\sum_{\boldsymbol{k}} \psi^\dagger_{\boldsymbol{k}+(\pi,\pi)}\psi_{\boldsymbol{k}} - 2m\sum_{\boldsymbol{k}}(\gamma_{\boldsymbol{k}} + \mu_d)\eta^\dagger_{\boldsymbol{k}+(\pi,\pi)}\eta_{\boldsymbol{k}}$ to H^{MF}_{tJ}, where $J^* = \lambda\tilde{J}$ and $\lambda = 0.31$ is a renormalization factor that enforces the transition between AF and SC orders at $x = 0.03$ on the HD side. [21] Without addressing the issue of coexistence of AF and SC, we obtain the AF phase shown in Fig. 1b. AF order is very robust on the ED side where it covers the pseudo-gap "Nernst" regime (labeled by N in Fig. 1b), in conformity with the absence of a vortex induced Nernst signal on these materials, [22] and extends over most of the SC dome.

To compare the above MF theory to ARPES we note that $c_{i,\sigma} = \frac{1}{\sqrt{2}}(d^\dagger_{i,\sigma} f^\dagger_{i,-\sigma} f_{i,-\sigma} f_{i,\sigma} f^\dagger_{i,\sigma} - d^\dagger_{i,-\sigma} f^\dagger_{i,\sigma} f_{i,-\sigma})$ is the electron annihilation operator and the electron creation operator in the HD and ED regimes respectively. Below we ignore the incoherent contribution to the electron spectral function and use $c_{i,\sigma} = \frac{1}{\sqrt{2}}(d^\dagger_{i,\sigma} + b_0 f^\dagger_{i,\sigma})$ instead. Figs. 2a-2c show how the MF electron spectral function along the nodal direction evolves with *hole* doping. These are $T = 0$ results and, thus, concern the SC phase. The spectral function mainly contains two peaks at $\epsilon^-_{1,\boldsymbol{k}}$ and $\epsilon^-_{2,\boldsymbol{k}}$ and displays the following behavior, which is also observed by ARPES: (a) In the underdoped regime two dispersive features arise. [4, 15] A linear dispersion crosses the Fermi level at a point that deviates from $(\frac{\pi}{2}, \frac{\pi}{2})$ toward $(0,0)$. At higher energy, a band that resembles the dispersion of the undoped AF samples carries most of the spectral weight. (b) The two dispersive features lead to a peak-dip-hump structure. [3, 4] (c) A nodal dispersion "kink" appears at the "dip" energy. [3] (d) Spectral weight is transfered, upon doping, from the $\epsilon^-_{2,\boldsymbol{k}}$ to the $\epsilon^-_{1,\boldsymbol{k}}$ band so that the low energy quasiparticle weight develops above the parent insulator dispersion (hence inside the Mott gap!). [15] (e) Increasing x weakens the AF correlations and reduces the spectral

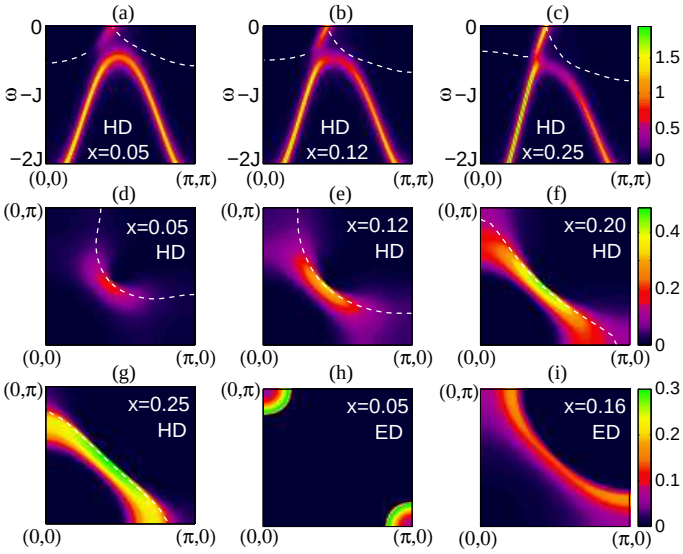

FIG. 2: Electron spectral weights at $T = 0$. (a)-(c) Evolution of the nodal direction *electron spectral function* with hole doping (top color scale). The white dashed line depicts the $\epsilon^-_{1,\boldsymbol{k}}$ band. (d)-(g) *Electron spectral weight* of the $\epsilon^-_{1,\boldsymbol{k}}$ band states for different x in the HD regime (middle color scale). The white dashed line represents the minimum gap locus. The maximum spectral weight for $x = 0.05, 0.12, 0.20, 0.25$ is 0.21, 0.35, 0.45 and 0.49 respectively. (h)-(i) *Integrated electron spectral weight* for $x = 0.05, 0.16$ in the ED regime (bottom color scale). The energy window $[-0.15J, 0.15J]$ was used. In (a)-(c) and (h)-(i) a Lorentzian broadening $\Sigma''(\omega) = \frac{J}{10}$ was used.

weight between the nodal point wavevector and (π,π). The "kink" gets smoothen out along this process. [17]

We remark that the spectral peak in the high energy $\epsilon^-_{2,\boldsymbol{k}}$ band is very sharp at MF level. However, beyond the MF approximation, the strong interaction between an electron in the $\epsilon^-_{2,\boldsymbol{k}}$ band and spinons in the $\epsilon^-_{1,\boldsymbol{k}}$ band may cause a fast decay of the electron (for instance, into an electron plus a pair of spinons). As a result, the spectral peak is expected to be very broad in the $\epsilon^-_{2,\boldsymbol{k}}$ band.

Figs. 2d-2g show how the spectral weight transfered from the high energy to the low energy band distributes in momentum space at $T = 0$ (hence in the SC phase). Notably, we find agreement with ARPES data: (a) The spectral weight associated with each state in the $\epsilon^-_{1,\boldsymbol{k}}$ band develops on top of an arc portion of the minimum gap locus. [4, 6] (b) A transition in the topology of the minimum gap locus from hole to electron-like at $x \approx 0.20$ is obtained. [5, 23, 24] (c) A two gap structure appears in underdoped samples. [3] Around the nodal point the dispersion is controlled by the d-wave SC gap of $\epsilon^-_{1,\boldsymbol{k}}$. Due to the vanishing of spectral weight in the $\epsilon^-_{1,\boldsymbol{k}}$ band near the anti-nodal points, the spectral structure in this $\boldsymbol{k}$-space region reflects only the high energy gap of $\epsilon^-_{2,\boldsymbol{k}}$ (which is reminiscent of the AF insulator). (d) The total spectral weight in the $\epsilon^-_{1,\boldsymbol{k}}$ band increases with doping as the arcs

extend to form a closed surface. (e) The coherence peaks in the anti-nodal region only appear around and beyond optimal doping. [2]

Figs. 2h and 2i show that the MF low energy electron spectral weight distribution for the ED regime is also consistent with experiments. Indeed, at $x = 0.05$ there is AF order and an electron pocket is formed around $(\pi, 0)$ and $(0, \pi)$. [16] Further doping induces SC order and the d-wave SC quasiparticles develop spectral weight in the nodal region. As a result, a large "Fermi surface", ungapped only along the nodal direction, is observed in Fig. 2(i). [16, 26]

To conclude, in this letter we introduce a new, fully fermionic, MF approximation to the $tt't''J$ model. Even though this model concerns an intrinsically one-band system, the MF approach gives an effective two-band description of the interplay between spin and charge dynamics. In the absence of spinon-dopon mixing the two bands separately describe the dynamics of the lattice spins and that of doped quasiparticles in a spin background with local AF correlations. Such a quasiparticle dynamics leads to the appearance of electron pockets in the AF phase of ED compounds around $(\pi, 0)$ and $(0, \pi)$ (Fig. 2h). [16] On the HD side, however, our calculations suggest that there are no hole pockets.

To understand this result we remark that local AF spin correlations strongly suppress the NN dopon hopping (in our MF approximation it is actually set to zero). Upon the spinon-dopon mixing mechanism, however, quasiparticles coherently hop between different sublattices. This fact shows up in the linear quasiparticle dispersion across the Fermi point [near $(\frac{\pi}{2}, \frac{\pi}{2})$] (Figs. 2a-2c). The kinetic energy gain that follows the emergence of NN hopping stabilizes the SC phase and the associated fractionalized spin-liquid background. [27] It also prevents the collapse of the chemical potential on top of the AF insulator band [15] once the dispersive features inherited from the undoped AF compounds (which show NN hopping frustration) are relegated to high energy. In our calculation the top of this band does not go above an energy $\approx -\frac{J}{2}$ even as $x \to 0$. This explains the lack of hole pockets, which agrees with experiments. [4, 15]

The dopon dynamics leads to several non-trivial spectral function features in the underdoped regime, all of which are fingerprints of the AF correlations in the metallic state. These are the nodal peak-dip-hump structure, the nodal dispersion "kink" and the Fermi arcs. We expect them to persist above T_c, as seen by experiments, [3, 4, 17] once they arise in the presence of a non-vanishing magnitude of the spinon-dopon mixing MF order parameters $b_{0,1}$. Right above T_c, in the Nernst region, we expect the arcs to be gapped everywhere but along the nodal direction, as the d-wave gap parameter $\Delta \neq 0$. Ungapped arcs can emerge, however, along the crossover between the Nernst and strange metal regimes.

The MF theory herein introduced provides a new route to the SC state via the coherent spinon-dopon mixing or, equivalently, the spinon-dopon pair condensation $\langle f_i^\dagger d_i \rangle \neq 0$. Above, we argue that this MF approach is relevant to both HD and ED cuprates. Indeed, we would like to stress that, even though the parameters in our MF theory are based on ARPES data, a relatively quantitatively correct phase diagram is obtained. Notably, this framework accounts for the peculiar evolution of the electronic structure from the undoped to the overdoped regime. Comparison to other experiments will appear in forthcoming publications.

The authors acknowledge conversations with P.A. Lee. This work was partially supported by the Fundação Calouste Gulbenkian Grant No. 58119 (Portugal). It is also supported by NSF Grant No. DMR–01–23156, NSF-MRSEC Grant No. DMR–02–13282, and NFSC no. 10228408.

[1] A. Damascelli *et al.*, Rev. Mod. Phys. **75**, 473 (2003).
[2] X.J. Zhou *et al.*, Phys. Rev. Lett. **92**, 187001 (2004).
[3] F. Ronning *et al.*, Phys. Rev. B **67**, 165101 (2003).
[4] Y. Kohsaka *et al.*, J. Phys. Soc. Jpn. **72**, 1018 (2003).
[5] A. Ino *et al.*, Phys. Rev. B **65**, 094504 (2002).
[6] T. Yoshida *et al.*, Phys. Rev. Lett. **91**, 027001 (2003).
[7] T. Tohyama *et al.*, J. Phys. Soc. Jpn. **69**, 9 (2000).
[8] W.-C. Lee *et al.*, Phys. Rev. Lett. **91**, 057001 (2003).
[9] T.C. Ribeiro, cond-mat/0409002.
[10] L. Krusin-Elbaum *et al.*, Phys. Rev. Lett. **92**, 097005 (2004). L. Krusin-Elbaum *et al.*, cond-mat/0405416 (2004).
[11] G.B. Martins *et al.*, Phys. Rev. B **60**, R3716 (1999).
[12] X.-G. Wen and P.A. Lee, Phys. Rev. Lett. **76**, 503 (1996).
[13] W. Rantner and X.-G. Wen, Phys. Rev. B **66**, 144501 (2002).
[14] C. Kane *et al.*, Phys. Rev. B **39**, 6880 (1989).
[15] K.M. Shen *et al.*, cond-mat/0407002 (2004).
[16] N.P. Armitage *et al.*, Phys. Rev. Lett. **88**, 257001 (2002).
[17] A. Lanzara *et al.*, Nature **412**, 510 (2001).
[18] P. Olsson, Phys. Rev. B **52**, 4526 (1995).
[19] N.P. Ong *et al.*, Annalen der Physik **13**, 9 (2004).
[20] I. Ussishkin *et al.*, Phys. Rev. Lett. **89**, 287001 (2002); I. Ussishkin and S.L. Sondhi, cond-mat/0406347 (2004).
[21] J. Brinckmann and P.A. Lee, Phys. Rev. B **65**, 014502 (2002).
[22] H. Balci *et al.*, Phys. Rev. B **68**, 054520 (2003).
[23] P.V. Bogdanov *et al.*, Phys. Rev. B **64**, 180505 (2001)
[24] Such a transition of topology is also obtained for the trial RVB wave function used in Ref. 25.
[25] C.T. Shih *et al.*, cond-mat/0401307 (2004).
[26] T. Claesson *et al.*, Phys. Rev. Lett. **93**, 136402 (2004).
[27] As first proposed by Anderson, [28] the optimization of the kinetic energy may force a RVB spin-liquid state in doped Mott insulators.
[28] P. W. Anderson, Science **235**, 1196 (1987).